

# The effect of in-plane deformations on the nonlinear dynamic response of laminated plates

Zafer Kazancı<sup>1a</sup> and Halit S. Turkmen\*<sup>2</sup>

<sup>1</sup>Aerospace Engineering Department, Turkish Air Force Academy, 34149, Yeşilyurt, Istanbul, Turkey

<sup>2</sup>Faculty of Aeronautics and Astronautics, Istanbul Technical University, 34469, Maslak, Istanbul, Turkey

(Received December 6, 2010, Revised February 15, 2012, Accepted April 24, 2012)

**Abstract.** In this study, the effect of in-plane deformations on the dynamic behavior of laminated plates is investigated. For this purpose, the displacement-time and strain-time histories obtained from the large deflection analysis of laminated plates are compared for the cases with and without including in-plane deformations. For the first one, in-plane stiffness and inertia effects are considered when formulating the dynamic response of the laminated composite plate subjected to the blast loading. Then, the problem is solved without considering the in-plane deformations. The geometric nonlinearity effects are taken into account by using the von Kármán large deflection theory of thin plates and transverse shear stresses are ignored for both cases. The equations of motion for the plate are derived by the use of the virtual work principle. Approximate solution functions are assumed for the space domain and substituted into the equations of motion. Then, the Galerkin method is used to obtain the nonlinear algebraic differential equations in the time domain. The effects of the magnitude of the blast load, the thickness of the plate and boundary conditions on the in-plane deformations are investigated.

**Keywords:** large deflection; blast loading; in-plane effects; laminated plate; geometric nonlinearity

---

## 1. Introduction

Laminated composite plates are widely used in several engineering fields such as space station structures, aircrafts, automobiles, ships, and submarines due to their high stiffness-to-weight and strength-to-weight ratios, long fatigue life, resistance to electrochemical corrosion. These structures are often subjected to large deformations because of their small thicknesses and geometrically nonlinear analyses are needed for more accurate solutions.

There are several studies on the static and dynamic large deflection analysis of plate and shell structures. In many of them, the in-plane effects are taken into account in the formulation of the problem. The static large deflection analysis of Reissner plate is achieved using the boundary element method including the in-plane effects (Dirgantara and Mohammadi 2006). In another study, the boundary element method is used to solve the large deflection of shell structures (Wen *et al.* 2005). In the mentioned study, the in-plane effects are also taken into account. The problem of large deflection including the transverse shear deformation effect is solved for the plates subjected to a

---

\*Corresponding author, Associate Professor, E-mail: [halit@itu.edu.tr](mailto:halit@itu.edu.tr)

<sup>a</sup>Assistant Professor

uniform lateral pressure (Liu *et al.* 1997). The large deflection analysis of laminated composite plates is performed using the layerwise displacement model (Cetkovic and Vuksanovic 2011). In the mentioned study, the nonlinear response of isotropic, orthotropic and anisotropic plates is calculated for different boundary and load conditions. The geometrically nonlinear free vibration problem of simply-supported thin circular plates is investigated considering the in-plane effects (Haterbouch and Benamar 2005). In another study, the geometrically nonlinear free vibration of fully clamped rectangular plates is investigated using a theoretical method based on Hamilton's principle (Harras and Benamar 2002). In the mentioned study, in-plane effects are not taken into account. The finite element method is also used to investigate the large deflection of plates considering the in-plane effects (Zhang and Kim 2006, Zhang and Yang 2006). In another numerical study, a meshless finite point method is used to solve the large deflection problem including the in-plane effects (Bitaraf and Mohammadi 2010).

The response of plates to air blast loading is also investigated by several researchers. The nonlinear damped vibrations of a laminated composite plate subject to a blast load are studied theoretically (Kazancı and Mecitoğlu 2006). The effect of aspect ratio and damping on the dynamic response of the plate are examined. It is found that the damping coefficient affects the nonlinear dynamic response. In another study of same researchers, in-plane stiffness and inertias in the analytical solution of the laminated composite plate under the blast load are considered (Kazancı *et al.* 2004). For the chosen problem, the displacement response of the plate follows the blast pressure and in-plane stiffnesses increase the frequency of the laminated plate in the first 20 ms that the blast pressure is quite high. The analytical-numerical approach on the large deflection analysis of unsymmetrically laminated composite plates is performed (Tanrıöver and Şenocak 2004). The problem of the dynamic response of sandwich panels exposed to blast loadings is addressed (Librescu *et al.* 2004, Kazancı 2011). Some experimental, analytical and numerical studies on the nonlinear structural response of laminated composites subjected to blast loading are performed (Turkmen and Mecitoğlu 1999a, b). The analysis of simply-supported orthotropic plates subject to the static and dynamic loads was presented (Dobyns 1981). In the study mentioned above, the response to the pulses of different shapes is analyzed. The response of stiffened and unstiffened plates subjected to blast loading is analyzed by using a single energy based formulation (Louca and Pan 1998). The dynamic response of the rectangular plates subjected to radial harmonic excitations are investigated by including the large deflection effects in the solution (Amabili 2004, 2006). The results obtained for the plates with different boundary conditions are compared to the experimental results and an agreement is found. The nonlinear response of elastic plates subjected to blast loading is investigated for simply-supported and clamped boundary conditions theoretically (Chandrasekharappa and Srirangarajan 1987). The effect of material damping, orthotropic parameter and aspect ratio on the dynamic response is investigated. It is found that increase in the material damping or decrease in the aspect ratio decreases the maximum deflection. The response of simply-supported anti-symmetrically laminated angle-ply plates to explosive blast loading is obtained using a closed-form solution (Birman and Bert 1987). They found that the decrease in the thickness results in the sharp increase of the maximum deflection. A semi-analytical finite strip method for the analysis of the nonlinear response to dynamic loading of simply-supported rectangular laminated composite plates is developed (Chen *et al.* 2000). It is found that the results are in an agreement with the finite element results. The results for nonlinear dynamic behavior of a laminated composite plate subjected to blast loading for different boundary conditions are compared (Kazancı and Mecitoğlu 2005). It is shown that the maximum normal strain of clamped plate occurs at a point

inside the plate after the peak positive pressure, during the vacuum phase. The maximum peak strain of the simply-supported plate is higher than that of the clamped one as expected. The nonlinear dynamic response of simply-supported laminated composite plates subjected to the blast load is investigated (Kazancı and Mecitoğlu 2008). The results of approximate numerical analysis are obtained and compared with the finite element results.

The objective of this study is to better understand the effect of in-plane deformations on the dynamic response of the laminated plate to the air blast loading. The effects of the load magnitude, plate thickness and boundary conditions on the dynamic response are also considered when investigating the effect of in-plane deformations on the plate response. For this purpose, two different formulations are used. In the first one, in-plane stiffness and inertia effects are considered when formulating the dynamic response of the laminated composite plate subjected to the blast loading. In the second one, the in-plane effects are not taken into account. In both of them, the geometric nonlinearity effects are taken into account by using the von Kármán large deflection theory of thin plates. Transverse shear stresses are ignored. The equations of motion for the plate are derived by the use of the virtual work principle. Approximate solution functions are assumed for the space domain and substituted into the equations of motion. Then, the Galerkin method is used to obtain the nonlinear algebraic differential equations in the time domain. A FORTRAN program was written to solve the nonlinear coupled equations of motion. The finite difference method is applied to solve the system of coupled nonlinear equations including in-plane effects. A Runge-Kutta-Verner method is used to solve the nonlinear equation without in-plane effects. The clamped and simply-supported boundary conditions are considered in both cases. A parametric study is also achieved to see the effect of positive phase duration and fiber orientation angle on the dynamic response of the laminated plate subjected to the blast load. The free vibration frequencies are calculated for the laminated plate with both simply-supported and clamped boundary conditions.

## 2. Equations of motion

In this section, a mathematical model for the laminated composite plate subjected to blast loading is shown in Fig. 1(a). The rectangular plate with the length  $a$ , the width  $b$ , and the thickness  $h$ , is considered. The Cartesian axes are used in the derivation. The strain-displacement relations for the von Kármán plate may be written as (Ventsel and Krauthammer 2001)

$$\varepsilon_x = \frac{\partial u^0}{\partial x} + \frac{1}{2} \left( \frac{\partial w^0}{\partial x} \right)^2 - z \frac{\partial^2 w^0}{\partial x^2} \tag{1a}$$

$$\varepsilon_y = \frac{\partial v^0}{\partial y} + \frac{1}{2} \left( \frac{\partial w^0}{\partial y} \right)^2 - z \frac{\partial^2 w^0}{\partial y^2} \tag{1b}$$

$$\varepsilon_{xy} = \frac{\partial u^0}{\partial y} + \frac{\partial v^0}{\partial x} + \frac{\partial w^0}{\partial x} \frac{\partial w^0}{\partial y} - 2z \frac{\partial^2 w^0}{\partial x \partial y} \tag{1c}$$

where  $u^0$ ,  $v^0$  and  $w^0$  are the displacement components in the  $x$ ,  $y$  and  $z$  directions. Force and moment components of the plate can be written as (Gibson 2007)

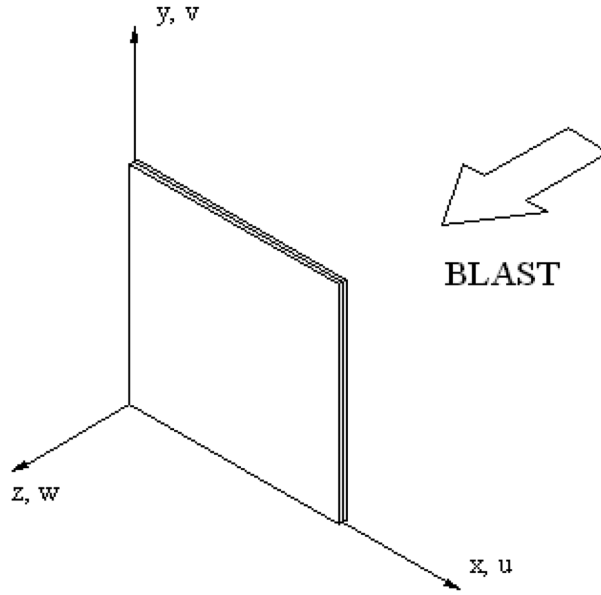


Fig. 1(a) Laminated composite plate subjected to blast load

$$\begin{Bmatrix} N_x \\ N_y \\ N_{xy} \\ M_x \\ M_y \\ M_{xy} \end{Bmatrix} = \begin{bmatrix} A_{11} & A_{12} & A_{16} & B_{11} & B_{12} & B_{16} \\ A_{12} & A_{22} & A_{26} & B_{12} & B_{22} & B_{26} \\ A_{16} & A_{26} & A_{66} & B_{16} & B_{26} & B_{66} \\ B_{11} & B_{12} & B_{16} & D_{11} & D_{12} & D_{16} \\ B_{12} & B_{22} & B_{26} & D_{12} & D_{22} & D_{26} \\ B_{16} & B_{26} & B_{66} & D_{16} & D_{26} & D_{66} \end{bmatrix} \begin{Bmatrix} \varepsilon_x^0 \\ \varepsilon_y^0 \\ \varepsilon_{xy}^0 \\ \kappa_x \\ \kappa_y \\ \kappa_{xy} \end{Bmatrix} \tag{2}$$

where  $\varepsilon_x^0, \varepsilon_y^0$  and  $\varepsilon_{xy}^0$  are the membrane strains and  $\kappa_x, \kappa_y$  and  $\kappa_{xy}$  are the curvatures and defined as

$$\varepsilon_x^0 = \frac{\partial u^0}{\partial x} + \frac{1}{2} \left( \frac{\partial w^0}{\partial x} \right)^2 \tag{3a}$$

$$\varepsilon_y^0 = \frac{\partial v^0}{\partial y} + \frac{1}{2} \left( \frac{\partial w^0}{\partial y} \right)^2 \tag{3b}$$

$$\varepsilon_{xy}^0 = \frac{\partial u^0}{\partial y} + \frac{\partial v^0}{\partial x} + \frac{\partial w^0}{\partial x} \frac{\partial w^0}{\partial y} \tag{3c}$$

$$\kappa_x = -\frac{\partial^2 w^0}{\partial x^2} \tag{4a}$$

$$\kappa_y = -\frac{\partial^2 w^0}{\partial y^2} \tag{4b}$$

$$\kappa_{xy} = -2\frac{\partial^2 w^0}{\partial x \partial y} \tag{4c}$$

The coefficients in the matrices are

$$A_{ij} = \sum_{k=1}^n (\bar{Q}_{ij})_k (h_k - h_{k-1}) \tag{5a}$$

$$B_{ij} = \frac{1}{2} \sum_{k=1}^n (\bar{Q}_{ij})_k (h_k^2 - h_{k-1}^2) \tag{5b}$$

$$D_{ij} = \frac{1}{3} \sum_{k=1}^n (\bar{Q}_{ij})_k (h_k^3 - h_{k-1}^3) \tag{5c}$$

where  $A_{ij}$ ,  $B_{ij}$ , and  $D_{ij}$  are the extensional, coupling and bending stiffness matrices, respectively.  $\bar{Q}_{ij}$ 's are the elastic constants for a laminate where  $h_k$  is the  $k$ th ply thickness.

Using the strain-displacement relations in the constitutive equations and the virtual work principles, nonlinear dynamic equations of a laminated composite plate can be obtained in terms of mid-plane displacements as follows

$$L_{11}u^0 + L_{12}v^0 + L_{13}w^0 + N_1(w^0) + \bar{m}\dot{u}^0 - q_x = 0 \tag{6a}$$

$$L_{21}u^0 + L_{22}v^0 + L_{23}w^0 + N_2(w^0) + \bar{m}\dot{v}^0 - q_y = 0 \tag{6b}$$

$$L_{31}u^0 + L_{32}v^0 + L_{33}w^0 + N_3(u^0, v^0, w^0) + \bar{m}\ddot{w}^0 - q_z = 0 \tag{6c}$$

where  $L_{ij}$  and  $N_i$  denote linear and nonlinear operators, respectively.  $\bar{m}$  is the mass of unit area of the mid-plane,  $q_x$ ,  $q_y$  and  $q_z$  are the load vectors in the axes directions. The dot denotes the derivative with respect to time. The explicit expressions of the operators can be found in Kazancı and Mecitoğlu (Kazancı and Mecitoğlu 2006, 2008). The damping terms are not included in this study. In a study on the nonlinear damped vibration of a laminated plate, it is found that damping effects are not observed during the time range of strong blast effect (Kazancı and Mecitoğlu 2006). The damping effects decrease the vibration amplitude in a short time afterwards. Therefore ignoring the damping effect may cause the over prediction of the vibration amplitude in the time range after the strong blast effect.

If the blast source is distant enough from the plate, the blast pressure can be described in terms of the Friedlander exponential decay equation (Gupta *et al.* 1987) as

$$P(t) = P_m(1 - t/t_p)e^{-\alpha t/t_p} \tag{7}$$

where the negative phase of the blast is included. In this equation,  $P_m$  is the peak blast pressure,  $t_p$  is the positive phase duration, and  $\alpha$  is the waveform parameter.

The boundary conditions can be given in the following form

$$\begin{aligned}
u^0(0, y, t) = u^0(a, y, t) = u^0(x, 0, t) = u^0(x, b, t) = 0 \\
v^0(0, y, t) = v^0(a, y, t) = v^0(x, 0, t) = v^0(x, b, t) = 0 \\
w^0(0, y, t) = w^0(a, y, t) = w^0(x, 0, t) = w^0(x, b, t) = 0
\end{aligned} \tag{8}$$

and initial conditions are

$$\begin{aligned}
u^0(x, y, 0) = 0, \quad v^0(x, y, 0) = 0, \quad w^0(x, y, 0) = 0 \\
\dot{u}^0(x, y, 0) = 0, \quad \dot{v}^0(x, y, 0) = 0, \quad \dot{w}^0(x, y, 0) = 0
\end{aligned} \tag{9}$$

In addition to the boundary conditions given above, the following boundary conditions apply for a simply-supported plate

$$\begin{aligned}
M_x = 0 \quad \text{at} \quad x = 0, a \\
M_y = 0 \quad \text{at} \quad y = 0, b
\end{aligned} \tag{10}$$

and, the following boundary conditions apply for a clamped plate

$$\begin{aligned}
\frac{\partial u^0}{\partial x}(0, y, t) = \frac{\partial u^0}{\partial x}(a, y, t) = \frac{\partial u^0}{\partial y}(x, 0, t) = \frac{\partial u^0}{\partial y}(x, b, t) = 0 \\
\frac{\partial v^0}{\partial x}(0, y, t) = \frac{\partial v^0}{\partial x}(a, y, t) = \frac{\partial v^0}{\partial y}(x, 0, t) = \frac{\partial v^0}{\partial y}(x, b, t) = 0 \\
\frac{\partial w^0}{\partial x}(0, y, t) = \frac{\partial w^0}{\partial x}(a, y, t) = \frac{\partial w^0}{\partial y}(x, 0, t) = \frac{\partial w^0}{\partial y}(x, b, t) = 0
\end{aligned} \tag{11}$$

### 3. Method of solution

The equations of motion given by Eq. (6) can be reduced into time domain by choosing some approximation functions for displacement field and applying the Galerkin method. The coupled-nonlinear equations in the time domain are solved by using the finite difference method. The approximation functions are selected so as to satisfy the natural boundary conditions.

$$u^0 = \sum_{i=1}^I \sum_{j=1}^J U_{ij}(t) \phi_{ij}(x, y) \tag{12a}$$

$$v^0 = \sum_{k=1}^K \sum_{l=1}^L V_{kl}(t) \psi_{kl}(x, y) \tag{12b}$$

$$w^0 = \sum_{m=1}^M \sum_{n=1}^N W_{mn}(t) \chi_{mn}(x, y) \tag{12c}$$

The simplest multi term approximations result in the hundreds of integral terms during the application of the Galerkin procedure and therefore they are impractical. Therefore, the approximation functions with single term for the displacement components are used in this study. As mentioned by Strang (1986), choosing the approximation functions is a crucial point. It should be most important for the single term solutions.

The approximation function should closely resemble the first mode of the plate. It can be determined by considering the results of the static large deformation analysis of laminated composite plate under the uniform pressure load by using ANSYS software as shown in the following forms (Kazancı and Mecitoğlu 2006, Kazancı 2009):

All edges simply-supported

$$\begin{aligned}
 u^0 &= U(t)\sin\frac{2\pi x}{a}y^2(y-b)^2 \\
 v^0 &= V(t)x^2(x-a)^2\sin\frac{2\pi y}{b} \\
 w^0 &= W(t)\sin\frac{\pi x}{a}\sin\frac{\pi y}{b}
 \end{aligned}
 \tag{13}$$

All edges clamped

$$\begin{aligned}
 u^0 &= U(t)x^2(x-a)^2\left(x-\frac{a}{2}\right)\left(1-\cos\frac{2\pi y}{b}\right) \\
 v^0 &= V(t)\left(1-\cos\frac{2\pi x}{a}\right)y^2(y-b)^2\left(y-\frac{b}{2}\right) \\
 w^0 &= W(t)\left(1-\cos\frac{2\pi x}{a}\right)\left(1-\cos\frac{2\pi y}{b}\right)
 \end{aligned}
 \tag{14}$$

Here,  $U$ ,  $V$ , and  $W$  denote the first term of the time-dependent parts of the solution functions  $u^0$ ,  $v^0$ , and  $w^0$ , respectively.

### 3.1 Case I: LDWI (Large deflection with in-plane effects)

Applying the Galerkin method to the equations of motion given in Eq. (6), the time dependent nonlinear algebraic differential equations can be obtained

$$a_0\ddot{U} + a_1U + a_2V + a_3W + a_4W^2 + a_5 = 0 \tag{15a}$$

$$b_0\ddot{V} + b_1V + b_2U + b_3W + b_4W^2 + b_5 = 0 \tag{15b}$$

$$c_0\ddot{W} + c_1W + c_2W^2 + c_3W^3 + c_4U + c_5V + c_6UW + c_7VW + c_8 = 0 \tag{15c}$$

The coefficients of the equations are given in (Kazancı and Mecitoğlu 2006, 2008). The initial conditions can be expressed as

$$U(0) = 0, \quad V(0) = 0, \quad W(0) = 0$$

$$\dot{U}(0) = 0, \quad \dot{V}(0) = 0, \quad \dot{W}(0) = 0$$

Nonlinear-coupled equations of motion are solved by using the finite difference method. We may arrange Eq. (15) in the matrix format as

$$[M]\{\ddot{Q}\} + [K_L]\{Q\} + [K_{NL}]\{Q\} + [F] = \{0\} \quad (16)$$

where  $\{Q\} = \{U \ V \ W\}^T$  and  $\{\ddot{Q}\} = \{\ddot{U} \ \ddot{V} \ \ddot{W}\}^T$  denote the displacement and acceleration vectors, respectively. In Eq (16),  $[M]$ ,  $[K_L]$  and  $[K_{NL}]$  matrices are

$$[M] = \begin{bmatrix} a_0 & 0 & 0 \\ 0 & b_0 & 0 \\ 0 & 0 & c_0 \end{bmatrix}, \quad [K_L] = \begin{bmatrix} a_1 & a_2 & a_3 \\ b_2 & b_1 & b_3 \\ c_4 & c_5 & c_1 \end{bmatrix}, \quad [K_{NL}] = \begin{bmatrix} 0 & 0 & a_4W \\ 0 & 0 & b_4W \\ c_6W & c_7W & (c_2W + c_3W^2) \end{bmatrix} \quad (17a)$$

and  $[F]$  vector is

$$\{F\} = \{a_5 \ b_5 \ c_8\}^T \quad (17b)$$

If we replace the  $\frac{\partial^2}{\partial t^2}\{Q\}$  term with  $\frac{\partial}{\partial t}\{\dot{Q}\}$  in Eq. (16), we can write down

$$[M]\frac{\partial}{\partial t}\{\dot{Q}\} + [K]\{Q\} + \{F\} = \{0\} \quad (18)$$

where  $[K] = [K_L] + [K_{NL}]$ .

Using the definition of derivation, the Eq. (18) can be written as

$$[M]\frac{\{\dot{Q}\}^{n+1} - \{\dot{Q}\}^n}{\Delta t} + [K]\{Q\}^{n+1} + \{F\} = \{0\} \quad (19)$$

Substituting  $\{\dot{Q}\}^{n+1} = \frac{\{Q\}^{n+1} - \{Q\}^n}{\Delta t}$  in Eq. (19) and rearranging it, we obtain

$$\left(\frac{1}{(\Delta t)^2}[M] + [K]\right)\{Q\}^{n+1} = \frac{1}{\Delta t}[M]\{\dot{Q}\}^n + \left(\frac{1}{(\Delta t)^2}[M]\right)\{Q\}^n - \{F\} \quad (20)$$

Finally, if the matrices and vector given in Eq. (17) are substituted into the Eq. (20), the equations of motion are reduced into

$$A_1U^{n+1} + A_2V^{n+1} + A_3W^{n+1} = A_4$$

$$B_1U^{n+1} + B_2V^{n+1} + B_3W^{n+1} = B_4$$

$$C_1U^{n+1} + C_2V^{n+1} + C_3W^{n+1} = V_4 \quad (21)$$

The coefficients in the equations are given in (Kazancı and Mecitoğlu 2006).

### 3.2 Case II: LD (Large deflection without in-plane effects)

In Eq. (15), if the in-plane inertias are ignored,  $U$  and  $V$  are calculated from the first two equations as zero and the equations of motion take the following form

$$c_0 \ddot{W} + c_1 \dot{W} + c_2 W^2 + c_3 W^3 + c_8 = 0 \tag{22}$$

The simply-supported and clamped boundary conditions are considered. Approximate solution functions chosen for the simply-supported and clamped boundary conditions are given in Eqs. (13) and (14), respectively. A code is written in FORTRAN for the approximate theoretical transient analysis of the laminated plates subjected to air blast loading. The fifth or sixth order Runge-Kutta-Verner method is used for the solution of nonlinear equation (Eq. (22)).

### 3.3 Finite element solution

The finite element model of the laminated plate subjected to the blast load is also created by using ANSYS finite element software. The plate is discretized using  $22 \times 22$  eight noded layered shell elements (Shell281) which have the geometric nonlinearity capability. The individual laminas are assumed to be perfectly bonded in the finite element model. The number of elements is chosen as  $22 \times 22$  based on the mesh sensitivity analysis. The air blast loading, given in Eq. (7), is applied on the plate. The transient analyses are performed to obtain the displacement-time histories at the central point of the plate. The finite element model of the plate is shown in Fig. 1(b).

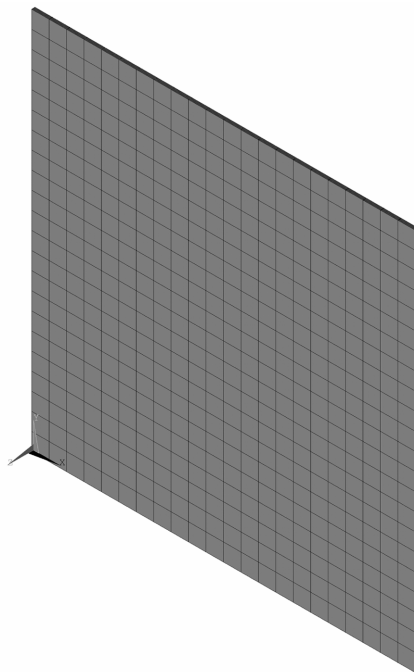


Fig. 1(b) Finite element model of the laminated plate

#### 4. Numerical results

Analyses are performed for three different laminated composites made of glass/epoxy. Ply material properties and fiber orientation angles used in the analyses are given in Table 1. M1 is the seven-layered bidirectional glass/epoxy with (0°/90°) fiber orientation angle for one layer. M2 and M3 are the seven-layered unidirectional glass/epoxy with the fiber orientation angles given in Table 1. The dimensions of the plate are  $a = 0.22$  m and  $b = 0.22$  m. The analyses are performed for the uniform blast pressure. The other parameters of the Friedlander's exponential decay function given in Eq. (7) are chosen as  $a = 0.35$  and  $t_p = 0.0018$  s. A parametric analysis is conducted to see the effect of peak pressure, boundary condition, thickness, positive phase duration and fiber orientation angle on the dynamic response of the laminated plate subjected to the blast load. The clamped and simply-supported boundary conditions are considered. Two different ply thicknesses are taken into account to see the effect of the thickness on the dynamic response of the plate. The ply thicknesses which are analyzed in this study are shown in Table 2. The loading conditions are shown in Table 3.

The displacement-time and strain-time histories of the plate center are obtained for three different pressure magnitudes, two different boundary conditions and plate thicknesses for M1. The central displacement-time and strain-time histories of the simply-supported plate are shown in Figs. 2-13. In these figures, one microstrain unit is equal to  $10^{-6}$  strain. The central displacement – time histories obtained by LDWI and LD analyses are almost same for the thickness T1 and Load Case I (Fig. 2).

Table 1 Properties of composite materials

Material	Bidirectional (M1) (0/90) <sub>7</sub>	Unidirectional (M2) (0/90/0/90/0/90/0)	Unidirectional (M3) (0/30/60/90/60/30/0)
$E_1$ (GPa)	24.14	40	40
$E_2$ (GPa)	24.14	10	10
$G_{12}$ (GPa)	3.79	4.5	4.5
$\nu_{12}$	0.11	0.27	0.27
$\rho$ (kg/m <sup>3</sup> )	1800	2000	2000

Table 2 Ply thicknesses (mm)

Case	Ply thickness (mm)	Total thickness (mm)
T1	0.56	$0.56 \times 7 = 3.92$
T2	0.28	$0.28 \times 7 = 1.96$

Table 3 Loading conditions.

Parameters	Load Case I	Load Case II	Load Case III
Pm (N/m <sup>2</sup> )	2890.6	28906	57812
$\alpha$	0.35	0.35	0.35
$t_p$ (s)	0.0018	0.0018	0.0018
Pressure distribution	uniform	uniform	uniform

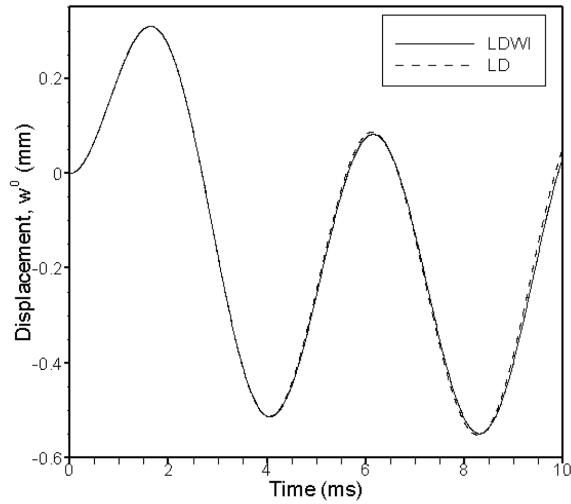


Fig. 2 Displacement time-history of simply-supported plate for thickness T1, Load Case I and M1

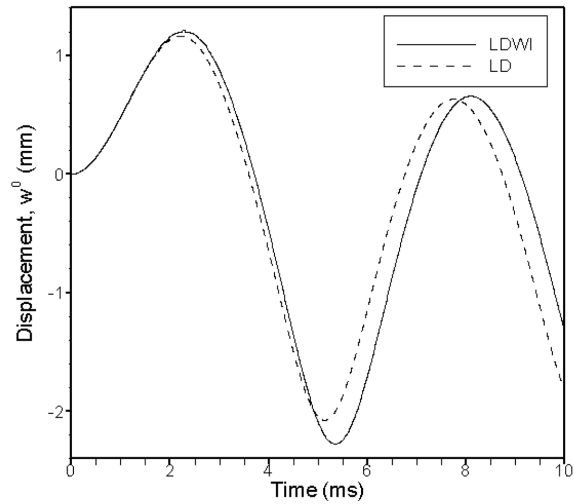


Fig. 3 Displacement time-history of simply-supported plate for thickness T2, Load Case I and M1

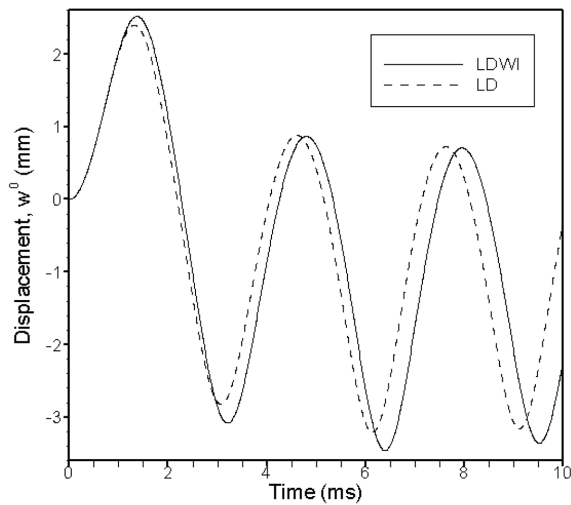


Fig. 4 Displacement time-history of simply-supported plate for thickness T1, Load Case II and M1

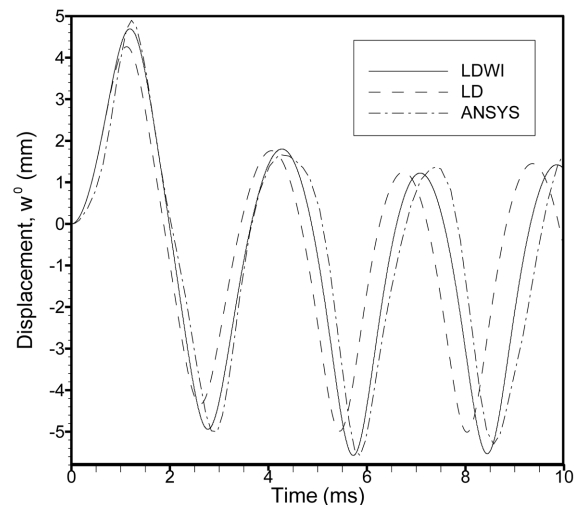


Fig. 5 Displacement time-history of simply-supported plate for thickness T2, Load Case II and M1

The predicted central displacements over the time are very close to each other for LDWI and LD cases for the simply-supported plate (Figs. 3-7). A slight difference occurs when the pressure is increased and the thickness is decreased because the effect of geometric nonlinearity increases. The displacement amplitude increases as the load is increased as expected. However, the increase in the displacement amplitude is not same as the load multiplication factor when the large deflection effect is pronounced (Figs. 3, 5, 7). The large deflection effect is much more pronounced for thinner plate (T2) and the highest load (LIII); the large deflection effect is less pronounced for thicker plate (T1) and the lowest load (LI). The plate behaves in the nonlinear manner when the large deflection effect

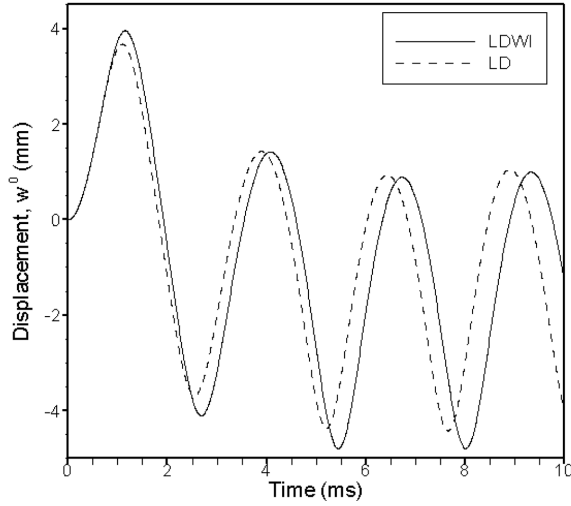


Fig. 6 Displacement time-history of simply-supported plate for thickness T1, Load Case III and M1

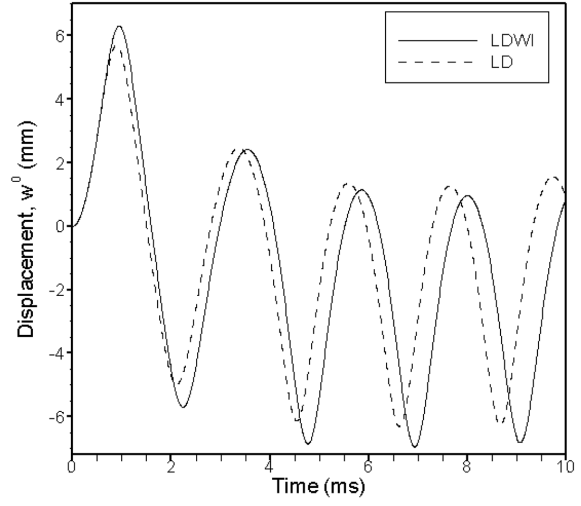


Fig. 7 Displacement time-history of simply-supported plate for thickness T2, Load Case III and M1

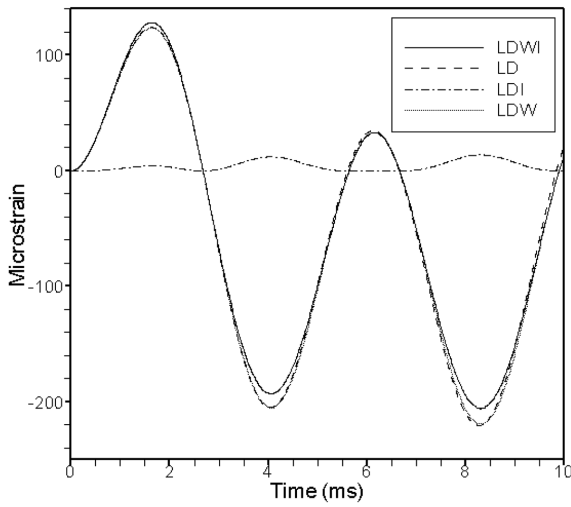


Fig. 8 Strain time-history of simply-supported plate for thickness T1, Load Case I and M1

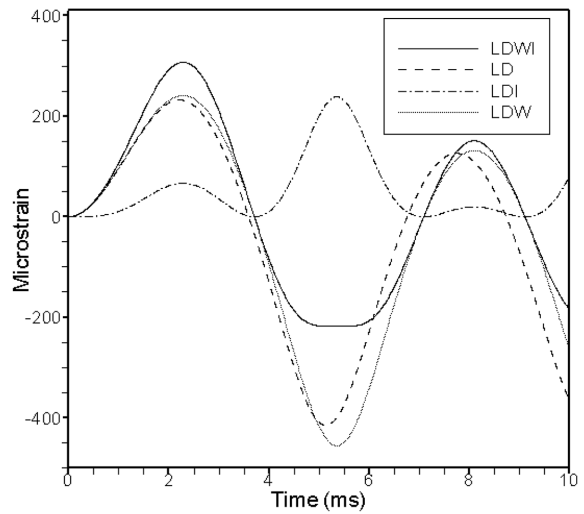


Fig. 9 Strain time-history of simply-supported plate for thickness T2, Load Case I and M1

is pronounced. The comparison of the displacement - time histories obtained by closed form solutions and the finite element method is given in Fig. 5. It is clearly shown that the LDWI and the finite element results are in an agreement. The strain-time histories give more detailed information on the effect of in-plane deformation on the response of the plate. A difference is shown between the predicted strain-time histories by LDWI and LD analyses (Figs. 8-13). This difference increases when the pressure magnitude is increased and the thickness is decreased. For the minimum pressure value and maximum plate thickness considered in this study, the plate behavior is in the linear range (Fig. 2). Therefore, the effect of in-plane deformations does not

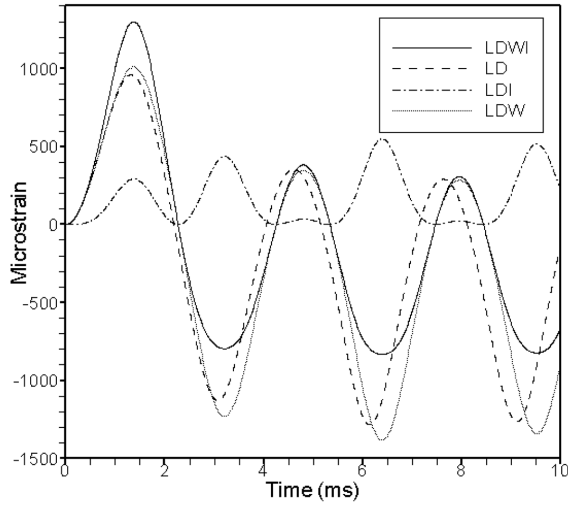


Fig. 10 Strain time-history of simply-supported plate for thickness T1, Load Case II and M1

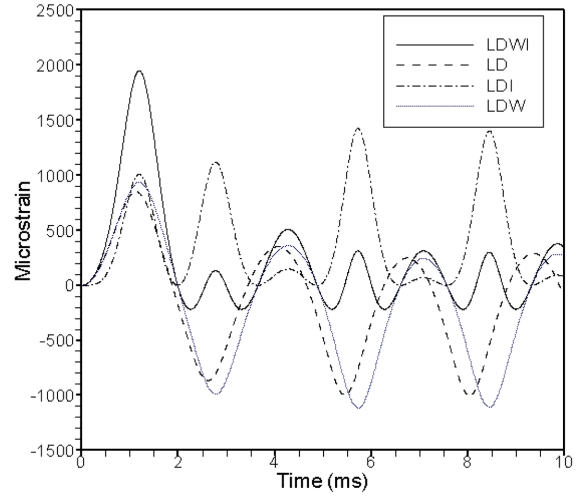


Fig. 11 Strain time-history of simply-supported plate for thickness T2, Load Case II and M1

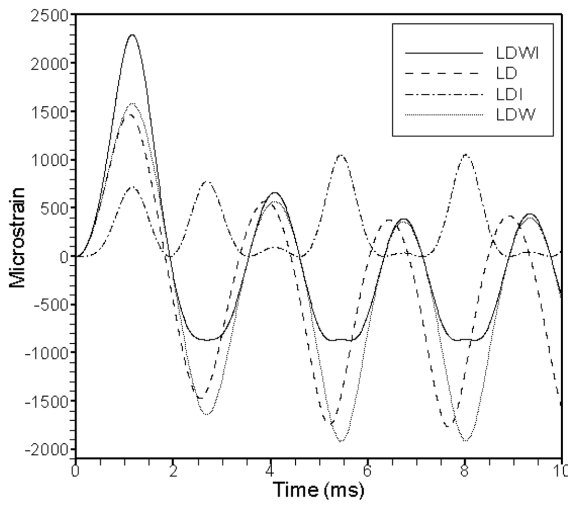


Fig. 12 Strain time-history of simply-supported plate for thickness T1, Load Case III and M1

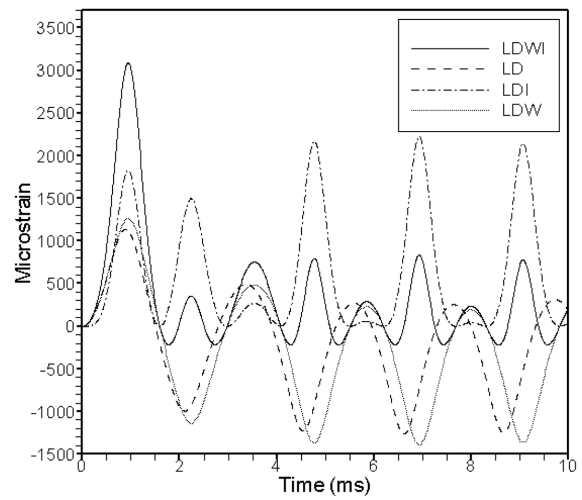


Fig. 13 Strain time-history of simply-supported plate for thickness T2, Load Case III and M1

appear (Fig. 8). The strain calculated by LDWI analysis could be separated in two portions. These are the strains because of the stretching of the plate (LDI) and bending of the plate (LDW). The first one is  $\varepsilon_x^0$  given in Eq. (3a) and expressed as stretching or membrane strain and the second one is  $-z\kappa_x$  given in Eq. (4a) and expressed as bending strain. The variations of these two strain components over the time are also presented in Figs. 8-13. It is clearly shown that the difference between LDWI and LD is close but not exactly same as the stretching portion of the strain. The comparison between the LD and LDW shows a slight difference that is indicating the bending strain will not be the same as the strain obtained by LD analysis. This is because the bending and

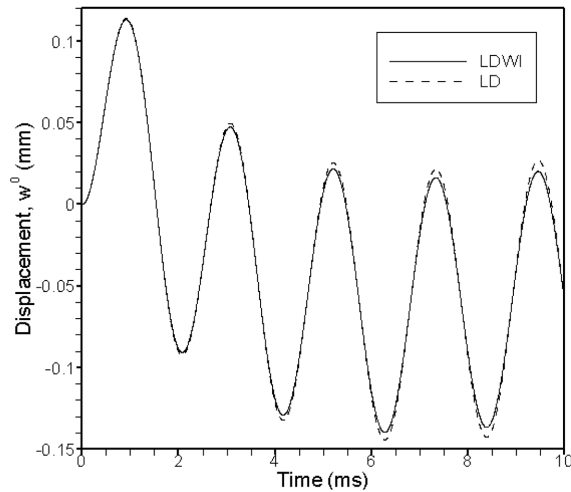


Fig. 14 Displacement time-history of clamped plate for thickness T1, Load Case I and M1

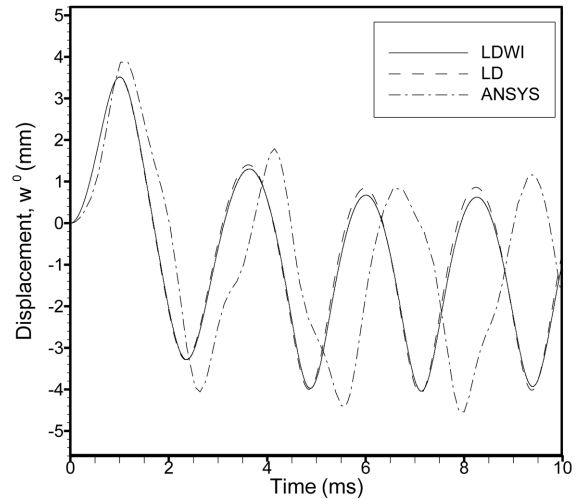


Fig. 15 Displacement time-history of clamped plate for thickness T2, Load Case II and M1

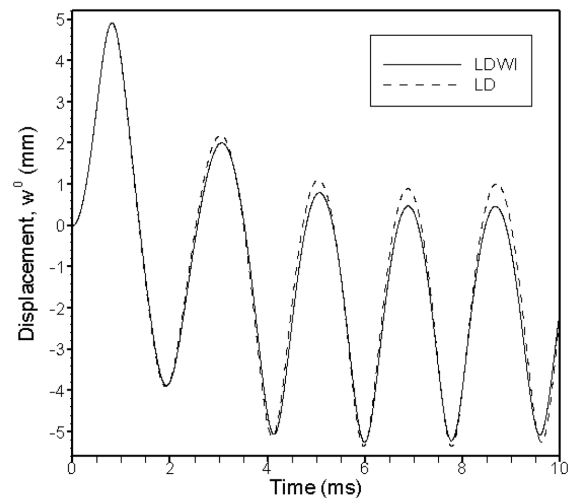


Fig. 16 Displacement time-history of clamped plate for thickness T2, Load Case III and M1

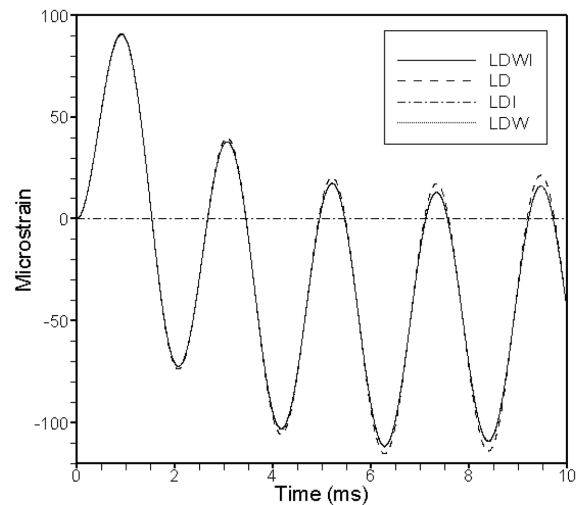


Fig. 17 Strain time-history of clamped plate for thickness T1, Load Case I and M1

stretching portions are coupled and this coupling influences the results.

The central displacement-time and strain-time histories of the clamped plate are shown in Figs. 14-19. The comparison between the LDWI and the finite element methods is given in Fig. 15 for T2 and LII. It is shown that the predicted values of displacements by LDWI analysis are found to be slightly lower than the FEM results and a shift occurs between two results after the first peak. This is because of the solution functions chosen for the in-plane and out-of-plane deformations. In this study, in-plane and out-of-plane deformations are described by using only the first term of the series solution. The solution function with one term cannot define the in-plane and out-of-plane

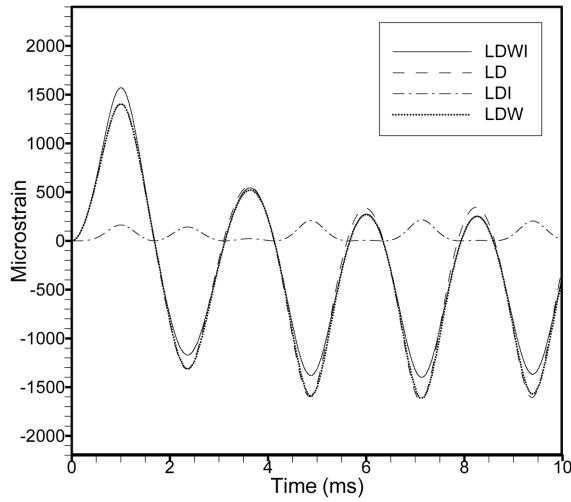


Fig. 18 Strain time-history of clamped plate for thickness T2, Load Case II and M1

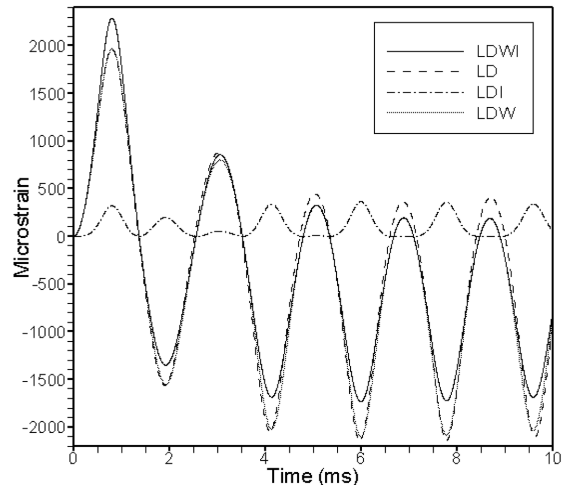


Fig. 19 Strain time-history of clamped plate for thickness T2, Load Case III and M1

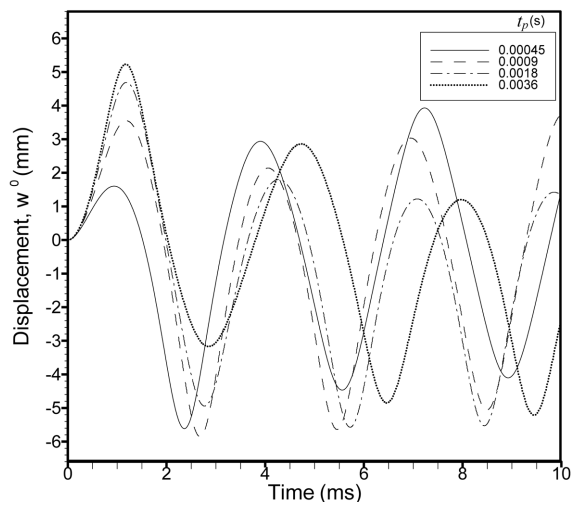


Fig. 20 The dependence of the displacement time-history on the positive phase duration for the simply-supported plate for thickness T2, Load Case II and M1

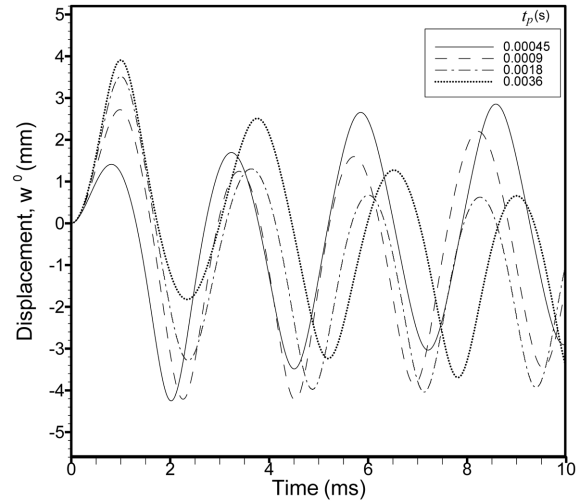


Fig. 21 The dependence of the displacement time-history on the positive phase duration for the clamped plate for thickness T2, Load Case II and M1

deformations exactly. The central displacement – time histories obtained by LDWI and LD analyses are almost same for the thickness T1 and Load Case I (Fig. 14). For the maximum plate thickness considered in this study, the plate behavior is in the linear range (Fig. 14). Therefore, the effect of in-plane deformations does not appear (Fig. 17). The predicted central displacements over the time obtained by LDWI analysis are slightly different from those obtained by LD analysis for the thickness T2 and Load Case III (Fig. 16). Even though the behavior of the plate is in the nonlinear

range for the thickness T2 and Load Case III (Fig. 16) a very small difference is observed between the predicted strain-time histories by LDWI and LD analyses (Fig. 19). The strain calculated by LDWI analysis could be separated in two portions as it is done for the simply-supported plate. These two strain variations over the time are also presented in Figs. 17-19. In general, LDI could be neglected for the clamped case. The stretching is higher for the simply-supported plate compared to the clamped plate. The large deflection effect is much more pronounced for the case of T2 and LIII, consequently the stretching becomes dominant. Therefore, the resistance of the simply-supported plate to the blast load increases more than the resistance of the clamped plate as the load is increased. Therefore, the effect of clamping becomes smaller for T2, LIII.

The analysis is performed for several positive phase durations to understand the effect of the period of the positive pressure load on the dynamic response of the plate. The higher peak displacement is obtained as the positive phase duration is increased for both simply-supported and clamped plates although the peak pressure is same for each case (Figs. 20 and 21). However, it is found that there is not a linear relation between the period of positive load and the increase in the peak displacement.

The free vibration frequencies of the laminated plate M1 are calculated for both simply-supported and clamped plates by using ANSYS finite element software. The vibration frequencies under blast effect (Figs. 2-7 and Figs. 14-16) are found to be closer to the free vibration frequencies of the first and second modes. This indicates that the first two modes are dominant for the vibration of the laminated plate subjected to the blast loading considered in this study. It is also observed that the vibration frequencies increase as the magnitude of the blast load is increased.

The displacement-time and strain-time histories of the plate center are obtained for the LIII, T2 and two different boundary conditions for M2 and M3. The central displacement-time and strain-time histories of the simply-supported plate are shown in Figs. 22-25. A slight difference is shown between the LDWI and LD cases for the displacements. A difference is shown between the

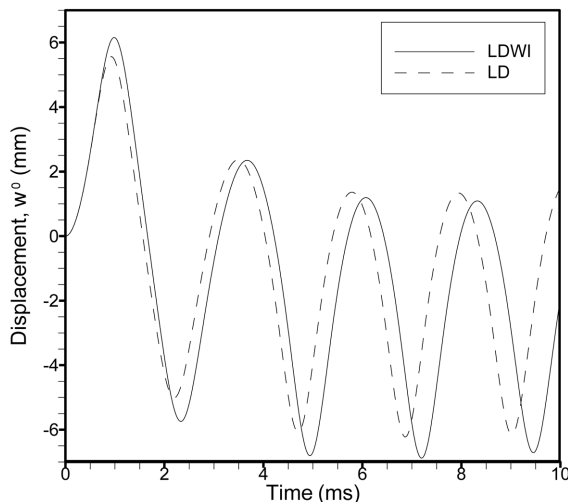


Fig. 22 Displacement time-history of simply-supported plate for thickness T2, Load Case III and M2

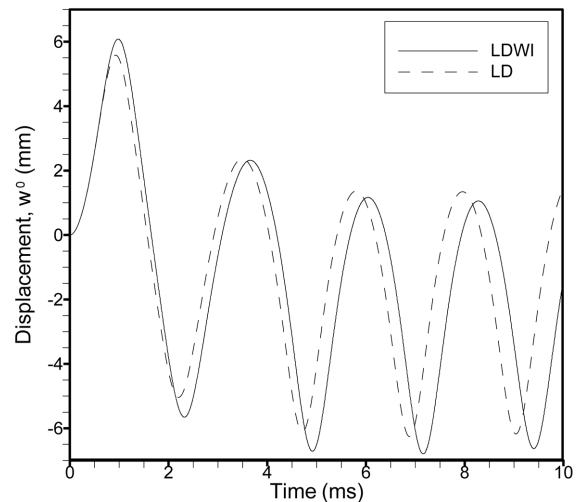


Fig. 23 Displacement time-history of simply-supported plate for thickness T2, Load Case III and M3

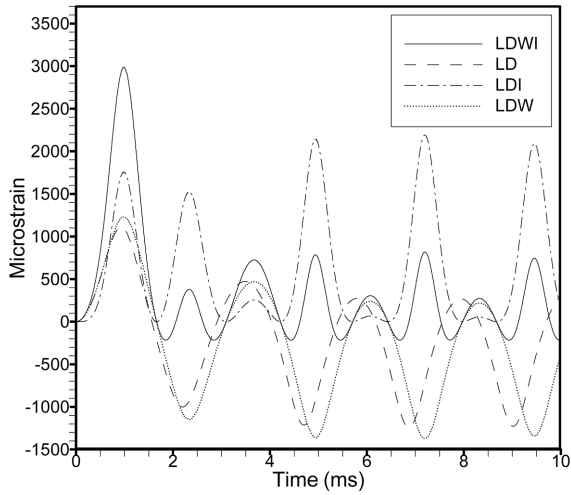


Fig. 24 Strain time-history of simply-supported plate for thickness T2, Load Case III and M2

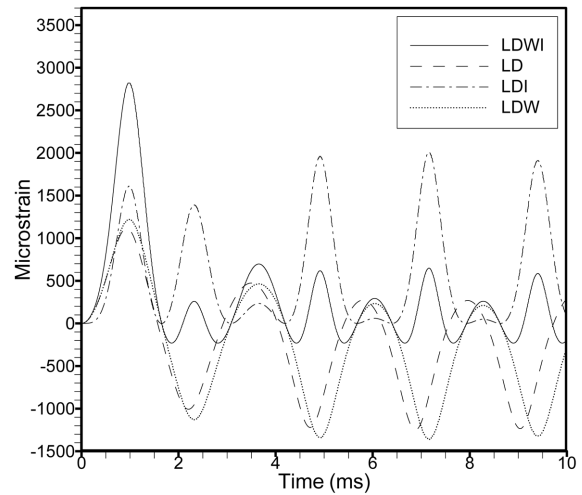


Fig. 25 Strain time-history of simply-supported plate for thickness T2, Load Case III and M3

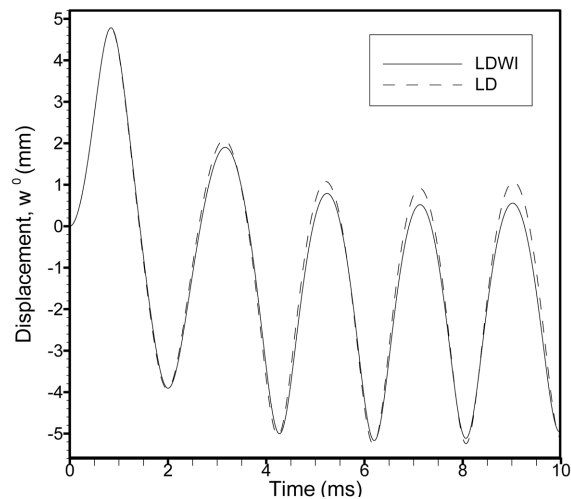


Fig. 26 Displacement time-history of clamped plate for thickness T2, Load Case III and M2

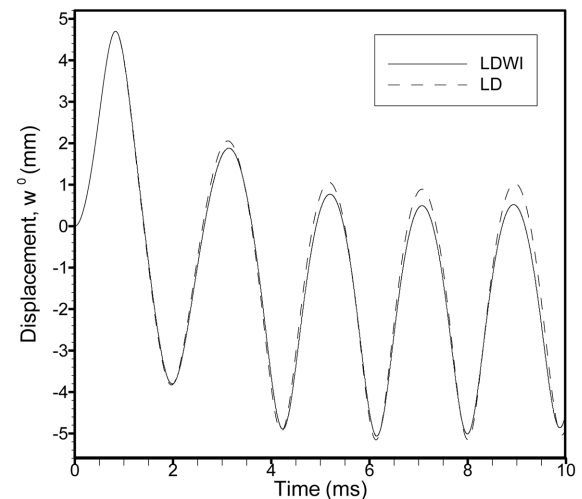


Fig. 27 Displacement time-history of clamped plate for thickness T2, Load Case III and M3

predicted strain-time histories by LDWI and LD analyses. Both the displacement amplitude and strain amplitude are found to be slightly higher for the M2 compared to those of M3. This indicates that the fiber orientation angles have an effect on the dynamic response of the plate and they could be chosen so that the maximum resistance to the blast load is obtained.

The central displacement-time and strain-time histories of the clamped plate are shown in Figs. 26-29. A slight difference is shown between the LDWI and LD cases for the displacements. A difference is shown between the predicted strain-time histories by LDWI and LD analyses. Similar to the simply-supported plate, both the displacement amplitude and strain amplitude are found to be

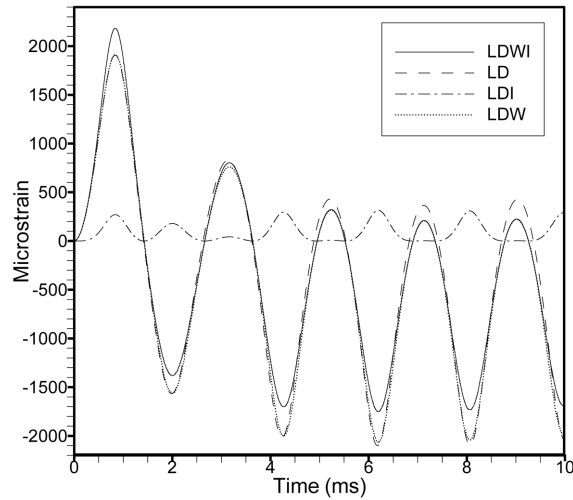


Fig. 28 Strain time-history of clamped plate for thickness T2, Load Case III and M2

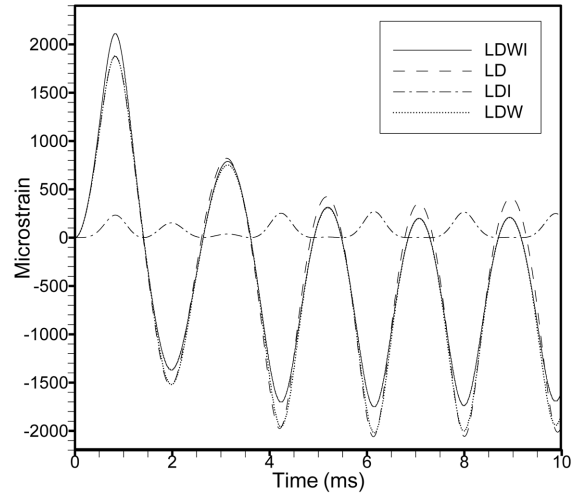


Fig. 29 Strain time-history of clamped plate for thickness T2, Load Case III and M3

Table 4 Free vibration frequencies of the laminated plate (M1)

Mode	Simply-supported (T1)	Simply-supported (T2)	Clamped (T1)	Clamped (T2)
1	113.33	224.67	228.76	449.83
2	303.24	597.62	468.30	907.77
3	303.24	597.62	468.30	907.77
4	451.41	884.21	654.38	1259.7
5	633.74	1233.3	852.72	1619.8

slightly higher for the M2 compared to those of M3. This indicates that the fiber orientation angles have an effect on the dynamic response of the plate and they could be chosen so that the maximum resistance to the blast load is obtained.

## 5. Conclusions

The predicted values of displacements are found to be slightly lower than the FEM results. This is the result of solution functions chosen for the in-plane and out-of-plane deformations. In this study, in-plane and out-of-plane deformations are described by using only the first term of the series solution. The solution function with one term cannot define the in-plane and out-of-plane deformations exactly. This can be a reason for the difference between two methods.

It is clearly shown that the stretching portion of the strain is higher for the simply-supported plates. This is because the edges of the simply-supported plate rotate during deformation. This

rotation causes the stretching of the plate an important amount in addition to the bending. This stretching increases as the load is increased. The increase in the load increases the nonlinearity. Therefore, it is important to consider the effect of in-plane deformations when the plate is simply-supported. However, in the case of clamped plate, the edges of the plate do not rotate; hence the stretching will be very small even the deformation is large. Therefore, the strain-time histories obtained from LD and LDWI analyses slightly differ. The displacement-time histories obtained from LD and LDWI analyses are close to each other for both simply-supported and clamped boundary conditions.

Another important result is that the bending portion of the strain is not exactly same as the strain obtained from LD analysis because of the coupling effect between stretching and bending during the solution. The parametric study on the effect of positive phase duration on the dynamic response indicates that there is not a linear relation between the increase in the peak displacement and the period of positive load. The free vibration frequencies of the laminated plate M1 are also calculated for both simply-supported and clamped plates by using ANSYS finite element software. It is observed that the first two modes are dominant for the vibration of the laminated plate subjected to the blast loading considered in this study.

## References

- Amabili, M. (2004), "Nonlinear vibrations of rectangular plates with different boundary conditions: theory and experiments", *Comput. Struct.*, **82**, 2587-2605.
- Amabili, M. (2006), "Theory and experiments for large-amplitude vibrations of rectangular plates with geometric imperfections", *J. Sound Vib.*, **291**, 539-565.
- Birman, V. and Bert, C.W. (1987), "Behaviour of laminated plates subjected to conventional blast", *Int. J. Impact Eng.*, **6**, 145-155.
- Bitaraf, M. and Mohammadi, S. (2010), "Large deflection analysis of flexible plates by the meshless finite point method", *Thin Wall Struct.*, **48**, 200-214.
- Cetkovic, M. and Vuksanovic, D. (2011), "Large deflection analysis of laminated composite plates using layerwise displacement model", *Struct. Eng. Mech.*, **40**, 257-277.
- Chandrasekharappa, G. and Srirangarajan, H.R. (1987), "Nonlinear response of elastic plates to pulse excitations", *Comput. Struct.*, **27**, 373-378.
- Chen, J., Dawe, D.J. and Wang, S. (2000), "Nonlinear transient analysis of rectangular composite laminated plates", *Compos. Struct.*, **49**, 129-139.
- Dirgantara, T. and Mohammadi, S.A. (2006), "Boundary element formulation for geometrically nonlinear analysis of shear deformable shells", *Comput. Meth. Appl. Mech. Eng.*, **195**, 4635-4654.
- Dobyns, A.L. (1981), "Analysis of simply-supported orthotropic plates subject to static and dynamic loads", *AIAA J.*, **19**, 642-650.
- Gibson, R.F. (2007), *Principles of Composite Material Mechanics*, CRC Press, Boca Raton.
- Gupta, A.D., Gregory, F.H., Bitting, R.L. and Bhattacharya, S. (1987), "Dynamic analysis of an explosively loaded hinged rectangular plate", *Comput. Struct.*, **26**, 339-344.
- Harras, B. and Benamar, R. (2002), "Geometrically non-linear free vibration of fully clamped symmetrically laminated rectangular composite plates", *J. Sound Vib.*, **251**(4), 579-619.
- Haterbouch, M. and Benamar, R. (2005), "Geometrically nonlinear free vibrations of simply supported isotropic thin circular plates", *J. Sound Vib.*, **280**, 903-924.
- Kazancı, Z., Mecitoğlu, Z. and Hacıoğlu, A. (2004), "Effect of in-plane stiffnesses and inertias on dynamic behavior of a laminated composite plate under blast load", *Proceedings of 9th Biennial ASCE Aerospace Division International Conference on Engineering, Construction, and Operations in Challenging Environments, Earth&Space-2004*, Houston, Texas, USA, March.

- Kazancı, Z. and Mecitoğlu, Z. (2005), "Nonlinear dynamic behavior of a laminated composite plate subject to blast load for different boundary conditions", *Ankara International Aerospace Conference (AIAC 2005)*, Ankara, Turkey, Paper AIAC 2005-044.
- Kazancı, Z. and Mecitoğlu, Z. (2006), "Nonlinear damped vibrations of a laminated composite plate subjected to blast load", *AIAA J.*, **44**, 2002-2008.
- Kazancı, Z. and Mecitoğlu, Z. (2008), "Nonlinear dynamic behavior of simply supported laminated composite plates subjected to blast load", *J. Sound Vib.*, **317**, 883-897.
- Kazancı, Z. (2009), "Nonlinear Transient response of a laminated composite plate under time-dependent pulses", *Proceedings of the 4th International Conference on Recent Advances in Space Technologies-RAST2009*, Istanbul, Turkey, June.
- Kazancı, Z. (2011), "Dynamic response of composite sandwich plates subjected to time-dependent pressure pulses", *Int. J. Nonlin. Mech.*, **46**, 807-817.
- Librescu, L., Oh, S.Y. and Hohe, J. (2004), "Linear and non-linear dynamic response of sandwich panels to blast loading", *Compos. Part B: Eng.*, **35**, 673-683.
- Liu, R.H., Xu, J.C. and Zhai, S.Z. (1997), "Large-deflection bending of symmetrically laminated rectilinearly orthotropic elliptical plates including transverse shear", *Arch. Appl. Mech.*, **67**(7), 507-520.
- Louca, L.A. and Pan, Y.G. (1998), "Response of stiffened and unstiffened plates subjected to blast loading", *Eng. Struct.*, **20**, 1079-1086.
- Strang, G. (1986), *Introduction to Applied Mathematics*, Wellesley-Cambridge Press, Wellesley, MA.
- Tanrıöver, H. and Şenocak, E. (2004), "Large deflection analysis of unsymmetrically laminated composite plates: analytical-numerical type approach", *Int. J. Nonlin. Mech.*, **39**, 1385-1392.
- Turkmen, H.S. and Mecitoğlu, Z. (1999a), "Nonlinear structural response of laminated composite plates subjected to blast loading", *AIAA J.*, **37**, 1639-1647.
- Turkmen, H.S. and Mecitoğlu, Z. (1999b), "Dynamic response of a stiffened laminated composite plate subjected to blast load", *J. Sound Vib.*, **221**, 371-389.
- Ventsel, E. and Krauthammer, T. (2001), *Thin Plates and Shells: Theory, Analysis, and Applications*, Marcel Dekker.
- Wen, P.H., Aliabadi, M.H. and Young, A. (2005), "Large deflection analysis of Reissner plate by boundary element method", *Comput. Struct.*, **83**, 870-879.
- Zhang, Y.X. and Kim, K.S. (2006), "Geometrically nonlinear analysis of laminated composite plates by two new displacement-based quadrilateral plate elements", *Compos. Struct.*, **72**, 301-310.
- Zhang, Y.X. and Yang, C.H. (2006), "A family of simple and robust finite elements for linear and geometrically nonlinear analysis of laminated composite plates", *Compos. Struct.*, **75**, 545-552.